Acta Montanistica Slovaca
ISSN 1335-1788
actamont.tuke.sk

Photocatalytic Degradation of Methylene Blue Using TiO2/Graphene Photocatalyst

Noor H. JABARULLAH[1]**, *Najwa ZAINUDDIN*[2], *Rapidah OTHMAN*[2], *Farra Wahida SHAARANI*[2] and *Wiesław LISZEWSKI*[3]

Authors' affiliations and addresses:
[1] Malaysian Institute of Aviation Technology, Universiti Kuala Lumpur, Sepang 43900, Malaysia
e-mail: nhafidzah@unikl.edu.my

[2] Chemical Engineering Section, Malaysian Institute of Chemical and Bioengineering, Universiti Kuala Lumpur, Melaka 78000, Malaysia
e-mail: najwazainuddin.02@s.unikl.edu.my;
e-mail: rapidah@unikl.edu.my;
e-mail: farrashaarani@unikl.edu.my

[3] Road and Bridge Research Institute, Instytutowa 1, Warsaw, 03-302, Poland
e-mail: wliszewski@ibdim.edu.pl

***Correspondence:**
Noor H. Jabarullah, Malaysian Institute of Aviation Technology, Universiti Kuala Lumpur, Sepang 43900, Malaysia
e-mail: nhafidzah@unikl.edu.my

Acknowledgement:
We would like to thank Universiti Kuala Lumpur Branch Malaysian Institute of Chemical and Bioengineering Technology (UniKL MICET) for all laboratory work and analysis.

How to cite this article:
Jabarullah, N.H., Zainuddin, N., Othman, R., Shaarani, F.W. and Liszewski, W. (2023), Photocatalytic Degradation of Methylene Blue Using TiO2/Graphene Photocatalyst, *Acta Monstanistica Slovaca,* Volume 28 (3), 765-778

DOI:
https://doi.org/10.46544/AMS.v28i3.19

Abstract
This study focused on the photocatalytic degradation of methylene blue (MB) under ultraviolet light irradiation. The photocatalyst used for methylene blue degradation was the composite of titanium dioxide and graphene, synthesized using the wet-impregnation method. The composition of TiO2/graphene was varied into three different mass ratios to characterize the composite further and identify the best photocatalyst for optimization. For each mass ratio, three affecting parameters, which were photocatalyst dosage, initial MB concentration and irradiation time, were employed to investigate the effects of degradation efficiency. Then, the statistical analysis for the photocatalytic degradation of MB using the most efficient TiO2/graphene photocatalyst was performed by utilizing the Response Surface Methodology.

Keywords
Photocatalytic degradation, Methylene blue, Titanium dioxide, Graphene, Wet-Impregnation, Response Surface Methodology.

Introduction

Methylthioninium chloride, or Methylene Blue (MB), is a cationic dye belonging to the phenothiazines family. It is a tricyclic phenothiazine that dissolves in water and some organic solvents (Juraj et al., 2021). Methylene blue (MB) is an organic dye that is widely utilized in plastics, textiles, and dye industries for multiple purposes. It has numerous beneficial properties for biomedical applications and acts as an effective therapeutic factor to treat anaemia, malaria, and Barrett's oesophagus (Dao et al., 2020). Despite its benefits, MB is one of the most abundant water pollutants that can cause adverse impacts on the aquatic environment since it has high potential toxicity and low degradation rate (L. Sun et al., 2019). Ensuring clean water is needed for sustainable development (Gaikward et al., 2010).

The degradation of MB cannot be done through conventional methods such as coagulation, adsorption and biological treatment due to its high stability against light irradiation, complex aromatic structures, hydrophilic nature, temperature, water and chemicals, which leads to substantial environmental pollution (Hou et al., 2018). However, photocatalysis is one of the most effective methods to remedy MB and remove phenolic compounds from wastewater solutions (Hana et al., 2022). It is a simple technique to treat wastewater which contains harmful pollutants (Muhd Julkapli et al., 2014). Previous work by Fang et al. found that the photocatalyst had exhibited an excellent performance in the pollutant's degradation with the help of light absorption in the water (Fang et al., 2017). Titanium dioxide, TiO2 has been demonstrated to be the most excellent photocatalyst in the treatment of environmental pollution, dye solar cells and biological applications due to its non-toxic nature, low cost and ability to possess charge transport properties and steady light absorption (Hou et al., 2018). However, TiO2 has a low utilization rate because of its large band gap of 3.0-3.2 eV, which can be excited using ultraviolet light with a wavelength shorter than 387 nm (H. Li et al., 2018). Therefore, various approaches have been applied to develop TiO2-based composites by incorporating TiO2 with non-metal, metal, or carbon-based materials to narrow down the band gap, elevate the light absorption spectrum and alter the density of electrons to avoid the recombination of charge carrier (Fang et al., 2017).

Incorporating graphene materials in TiO2 resulted in a good absorbent to remove the organic pollutants due to electrostatic attraction, high adsorption of light, $\pi-\pi$ interaction and high electron mobility (Chen et al., 2020). Graphene, which is an atom-thick sheet of sp2-hybridized carbon, has gained significant attention in the field of photocatalysis due to its favourable bandgap and outstanding electrical and electronic properties (Nasir et al., 2020). The presence of graphene in the composite improved the adsorption ability of TiO2 and reduced the recombination of charge carriers, resulting in photocatalytic efficiency enhancement. Moreover, graphene has a high mobility of charge carriers and a large specific surface area, which acts as a good support for semiconductor photocatalysts (Khalid et al., 2017).

The wet impregnation technique has been selected for the synthesis of TiO2/graphene composites in this study due to its simplicity and inexpensive method, which can be performed in a short time and allows the final properties as well as the configuration of the photocatalysts to be controllable in advance (Durango-Giraldo et al., 2019). In this method, graphene as a support was impregnated with TiO2 in a methanol solution and was then sintered at high temperatures to activate the photocatalyst. Response Surface Methodology (RSM) was utilized to design experiments and analyze the effects of operating parameters to determine ideal conditions. RSM is a collection of statistical and mathematical methods that can be employed to create empirical models, design experiments and study the effects of operational parameters. This method is practical in considering the interaction between operating parameters and, subsequently, is able to determine the significant ideal experimental conditions precisely with the least amount of work.

In this study, three operational parameters were used (photocatalyst dosage, initial concentration of MB and irradiation time) to analyze the optimum operating parameters for MB degradation using different ratios of TiO2/graphene photocatalyst. This study not only provides numerous advantages to the application of effective photocatalysts but also enhances the performance and materials utilization throughout the photocatalysis process.

Materials and methods

Synthesis of TiO_2/graphene

The synthesis of TiO_2/graphene composite was conducted via the wet impregnation method into three different mass ratios of TiO_2 to graphene. The preparation was started by mixing graphene with 100 ml of methanol containing TiO_2. Then, the mixture was ultrasonicated for 30 minutes to obtain uniform dispersion. After that, the solution was agitated constantly at 600 rpm and heated to 80°C for 3 hours to remove the adsorbed liquid. After methanol was completely vaporized, the TiO_2/graphene composite was sintered at 300ºC in a furnace for 2 hours. The synthesized photocatalysts were designated as TiO_2, TiO_2/graphene-M2 and TiO_2/graphene-M3 for the ratio of TiO2/graphene 100:0, 50:50 and 25:75, respectively. **Chyba! Nenašiel sa žiaden zdroj odkazov.** s hows the photocatalyst prepared based on different mass ratios.

Tab. 1. Sample label of photocatalyst based on different mass ratios

No	**Sample label**	**TiO_2 to graphene mass ratio**
1	TiO_2	100:0
2	TiO_2/graphene-M2	50:50
3	TiO_2/graphene-M3	75:25

Characterization of photocatalyst

The functionality groups of the samples were determined using an FTIR spectrophotometer (NICOLET iS10, Thermo Scientific). Prior to FTIR analysis, the photocatalyst was blended with potassium bromide (KBr) to obtain the pellets and the region of spectroscopy used will be in the range of 500 to 4000 cm^{-1}. The XRD analysis was conducted using Bruker-Axs D8 Advance instrument, in the 2θ range of 10°–80° at a scanning rate of 0.02° s^{-1} to determine the crystalline properties.

Photocatalytic degradation of MB

The photocatalytic activities of the samples were evaluated via the photocatalytic oxidation of MB under UV light irradiation. The 8W UV lamp was used as a light source. The photocatalyst dosage, the initial concentration of MB and irradiation time were the operating parameters studied. The initial values of each parameter were used as a reference for the adjustment of the affected parameter, as shown in Tab. .

Tab. 2. Initial values of each parameter as reference for the adjustment of the affected parameter

Parameter	Value
Photocatalyst dosage	0.2 g/L
Initial concentration of methylene blue	20 ppm
Irradiation time	90 minutes

Before the irradiation, the MB photocatalytic degradation was conducted in a 250 mL beaker that acts as a reactor. The reaction mixture in the reactor was stirred uniformly for 30 minutes using a magnetic stirrer to produce a homogenous mixture. During the mixing, the beaker was placed in a closed container to keep the samples in the dark without any light exposure.

To study the first parameter, 100 mL MB solution was prepared in a beaker with 20 ppm of MB initial concentration. The photocatalyst dosage of TiO2/graphene varied to 0.2 g/L, 0.3 g/L and 0.4 g/L. The beaker was placed in a closed container to keep the samples in the dark without any light exposure. The solution was stirred continuously using a magnetic stirrer for 30 minutes to reach an adsorption equilibrium of MB on the photocatalyst surface. The time was recorded as soon as the light was turned on, and the irradiation time was set to be 90 minutes. Similar steps were repeated using samples of TiO2/graphene-M2 and TiO2/graphene-M3. Subsequently, the photocatalyst dosage that achieved the highest efficiency of MB degradation was set as a constant parameter to study the influence of MB initial concentration. The previous steps were repeated for the other three samples by varying the concentration of 20 ppm, 25 ppm and 30 ppm at 90 minutes.

Finally, to measure the effects of irradiation time, the values were varied to 60 minutes, 90 minutes and 120 minutes. However, based on previous studies, the photocatalyst dosage and initial concentration of MB were kept constant at their respective optimum values for each photocatalyst. Then, the results collected from the experiment were compared and discussed for further analysis. Tables 3a, 3b and 3c listed the samples together with their operational conditions for three parameters, including photocatalyst dosage, MB initial concentration and irradiation time, respectively.

Tab. 3a. Photocatalyst samples to study the effects on photocatalyst dosage

Effects on photocatalyst dosage				
Photocatalysts	Sample	Photocatalyst dosage (g/L)	Initial concentration of MB (ppm)	Irradiation time (min)
TiO_2	A1	0.2	20	90
	A2	0.3		
	A3	0.4		

TiO_2/Graphene-M2 (50:50)	B1	0.2	20	90
	B2	0.3		
	B3	0.4		
TiO_2/Graphene-M3 (75:25)	C1	0.2	20	90
	C2	0.3		
	C3	0.4		

Tab. 3b. Photocatalyst samples to study the effects on MB initial concentration

Effects on MB initial concentration				
Photocatalysts	Sample	Photocatalyst dosage (g/L)	Initial concentration of MB (ppm)	Irradiation time (min)
TiO_2	A1	0.4	20	90
	A2		25	
	A3		30	
TiO_2/Graphene-M2 (50:50)	B1	0.3	20	90
	B2		25	
	B3		30	
TiO_2/Graphene-M3 (75:25)	C1	0.3	20	90
	C2		25	
	C3		30	

Tab. 3c. Photocatalyst samples to study the effects on irradiation time

Effects on irradiation time				
Photocatalysts	Sample	Photocatalyst dosage (g/L)	Initial concentration of MB (ppm)	Irradiation time (min)
TiO_2	A1	0.4	30	60
	A2			90
	A3			120
TiO_2/Graphene-M2 (50:50)	B1	0.3	20	60
	B2			90
	B3			120
TiO_2/Graphene-M3 (75:25)	C1	0.3	20	60
	C2			90
	C3			120

The degradation efficiency of MB was analyzed using a UV-Vis spectrometer (Model UV-1900i by Shimadzu Corp.). The peaks were observed to be present between 600 and 700 nm and were assigned as the absorption of the π-system, which was indicative of the MB degradation. Based on Beer-Lambert Law, the concentration of MB is directly proportional to its absorbance. By applying this law, it was possible to determine the efficiency of MB degradation using Equation 1:

$$\frac{C_0 - C_f}{C_0} \times 100\% \tag{1}$$

where C_o is the initial concentration of MB solution, and C_{f} is the final concentration of MB.

Experimental design of MB photocatalytic degradation

The Central Composite Design (CCD) of RSM was utilized to analyze the interaction among three operational factors: photocatalyst dosage, MB initial concentration and irradiation time to achieve an optimum degradation rate of MB. The photocatalyst with the highest degradation efficiency from the preliminary experiment was selected for the statistical analysis. In this study, Design Expert version 13 was used to design experiments and study the interactions among these operating factors with a total of 20 runs, as shown in Table 4.

Tab. 4. 20 sets of experimental designs that the CCD by RSM developed

Run	Photocatalyst dosage (g/L)	Initial concentration MB (ppm)	Irradiation time (min)
1	0.2	30	120
2	0.4	30	60
3	0.3	25	90
4	0.3	16.59	90
5	0.4	20	120
6	0.2	20	60
7	0.3	25	90
8	0.4	20	60
9	0.3	25	90
10	0.2	30	60
11	0.3	25	90
12	0.47	25	90
13	0.3	25	39.55
14	0.2	20	120
15	0.3	25	140.45
16	0.13	25	90
17	0.3	25	90
18	0.3	25	90
19	0.4	30	120
20	0.3	33.41	90

Results

Characterization of photocatalyst
FTIR Analysis

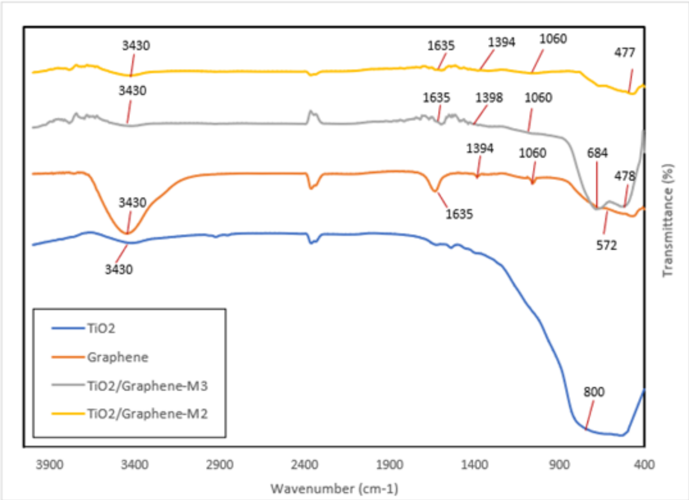

Fig. 1. FTIR spectra of TiO2, graphene and their composites

The characteristic functional groups and chemical bonds in the synthesized photocatalyst were determined from FTIR spectra. Fig 1 depicts the FTIR spectra of TiO2, graphene and two different TiO2/graphene composites that were derived from the wet-impregnation method.

It can be observed that typical IR spectrum of graphene showed broad band of the stretching vibration of hydroxyl (-OH) groups near 3430 cm^{-1} due to water molecules absorption, at 1635 cm^{-1} was attributed to bending vibration peak of C=O in graphene, at 1384 cm^{-1} was assigned to the stretching vibration peak of C-OH bonds and a vibration absorption peak was present at 1060 cm^{-1} which represented C-O-C bonds (Y. Li et al. 2020; Liu et al. 2016; Nasir et al., 2020). The oxygen-containing functional groups served as hole traps to facilitate the charge transfer to prevent the recombination of electron-hole pairs and hence improved the conductivity activity (M. Sun et al., 2017). These results indicated that these functional groups of oxygen, such as -OH, C=O, C-OH and C-O-C on the graphene's surface, strengthen the bonding between TiO2 and graphene (Y. Li et al., 2020). As for TiO2, it had a wide and strong absorption peak at the region near 800 cm^{-1}, which happened due to the stretching of Ti-O-Ti bonds. Similar to graphene, the band attributed to the OH group is also present near 3430 cm^{-1} (Nasir et al., 2022). In addition, it was observed that the characteristic absorption peak near 478 cm^{-1} was caused by the presence of a Ti-O-C bond. This implied a successful combination of TiO2 and graphene by using the wet-impregnation method. However, the characteristic bands of graphene and TiO2 in TiO2/graphene composites were relatively weaker or almost removed, resulting in smaller FTIR spectra peaks (Nasir et al., 2022). It can be proven in the figure as the intensity of peaks at 3430 cm^{-1}, 1635 cm^{-1}, 1394 cm^{-1}, and 1060 cm^{-1} of TiO2/graphene composites were weaker. The differences in peaks' intensity might be due to the absorption intensity of oxygen-containing functional groups on graphene's surface being reduced by the chemical interaction of TiO2 with graphene (Y. Li et al., 2020). The TiO2/graphene-M2 showed a high intensity of peaks compared to TiO2/graphene-M3 due to the higher mass ratio of graphene.

In TiO2/graphene-M2, the peaks of the main functional groups in graphene, such as OH-groups and C=C, were higher, but Ti-O-Ti peaks were less intense compared to TiO2/graphene-M3. Since the mass ratio of graphene to TiO2 in the M3 photocatalyst is smaller than TiO2/graphene-M2, the functional groups of graphene were retained with a significant decrease in peak intensity, whereas the presence of Ti-O-Ti bonds were shown prominently. This was in accordance with the studies reported by Nasir (2020).

XRD Analysis

XRD analysis was applied to examine the crystalline structure and phase of the synthesized photocatalyst. Fig 2 shows the XRD patterns of the prepared samples of TiO2, graphene and TiO2/graphene photocatalysts at different mass ratios. In the samples containing TiO2 (TiO2, TiO2/graphene-M2, TiO2/graphene-M3), the main diffraction peaks were at 25.27o, 37.86o, 48.06o, 53.96o, 55.02o, 62.67o which correspond to the diffraction planes (101), (004), (200), (105), (211) and (204) for anatase TiO2 (JCPCDS card 21-1272) (Amali et al., 2014). The similarities between the observed and standard values proved that the TiO2 used was pure anatase TiO2 with a tetragonal structure because of the strong diffraction peaks at 25° and 48° (Najafi et al., 2017).

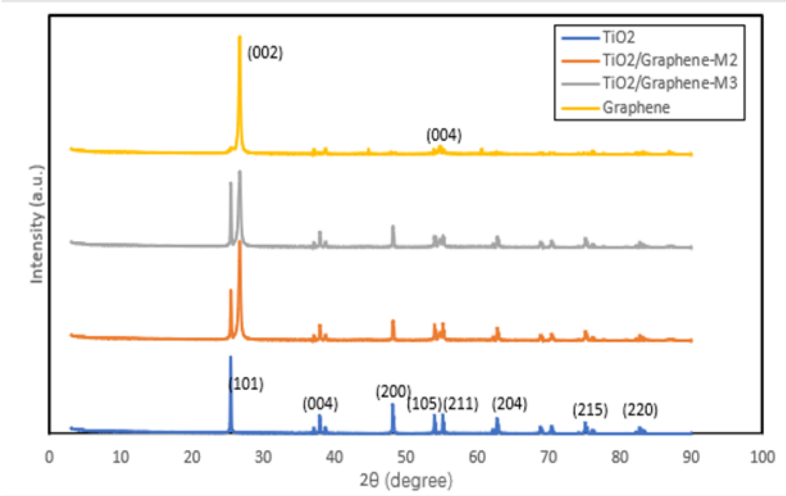

Fig. 2. XRD spectra of TiO2, graphene and their composites

As for graphene, the appearance of peaks at 25.50o corresponds to a similar diffraction plane of (002), which clearly demonstrates the characteristics peak correlating to the crystal layer of graphene (Mahalingam et al., 2021). The appearance of the (004) diffraction peak implied the good crystallinity of the material, which indicates a greater average number of graphene stacked (Ouyang et al., 2014). In addition, XRD showed that the binding of graphene to TiO2's surface did not influence the crystalline structure of TiO2. However, the intensity of diffraction peaks became lower, especially for TiO2/graphene-M3. This can be explained by the smaller TiO2 peaks in TiO2/graphene-M3 compared to TiO2/graphene-M2 due to the higher mass ratio of TiO2 to graphene in TiO2/graphene-M3 photocatalyst (75:25). Overall, it can be concluded that the sintering temperature at 300oC during the synthesis of the TiO2/graphene photocatalysts did not disrupt the crystalline structure of photocatalysts.

Photocatalytic degradation of MB
Effects of photocatalyst dosage

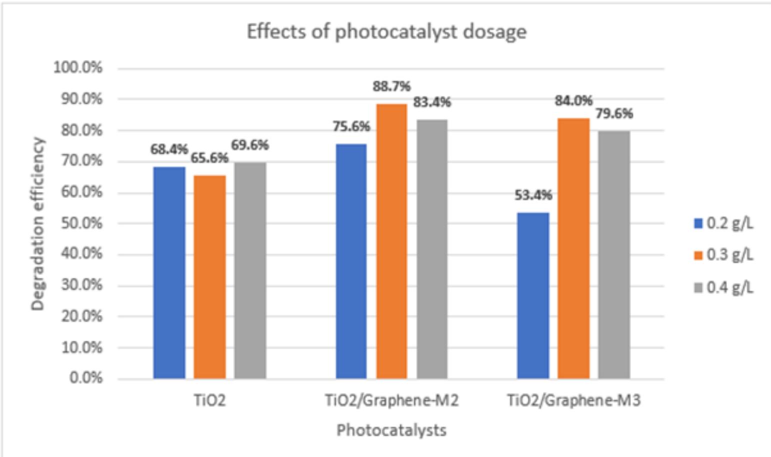

Fig. 3. Photocatalytic degradation by TiO2 and TiO2/graphene composites for different photocatalyst dosage

Fig 3 illustrates the effect of photocatalyst dosage on MB degradation efficiency for different photocatalysts. For TiO2, the dosage of 0.4 g/L exhibited the highest efficiency (69.6%), while the lowest efficiency was at 0.3 g/L (65.6%). Next, for TiO2/graphene-M2, the degradation efficiency of MB was increased from 75.6% to 88.7% as the dosage was increased up to 0.3 g/L but then decreased to 83.7% when the dosage was above 0.4 g/L. TiO2/graphene-M3 showed the same trend as TiO2/graphene-M2 as the efficiency of MB degradation was also increased from 53.4% to 84% as the photocatalyst dosage increased, which then decreased to 79.6% as the dosage increased to 0.4 g/L. Increasing the photocatalyst dosage resulted in the increment of the total catalyst surface area, which leads to the formation of more active sites on the photocatalyst surface (Abdel-Khalek et al., 2018). This enhances the adsorption rate of photons and the formation of hydroxyl species, resulting in higher efficiency of MB degradation (Zhang et al., 2018). As the dosage of TiO2/graphene-M2 and TiO2/graphene-M3 were increased above 0.3 g/L, the degradation efficiency of MB was reduced. This is because an excess loading of the photocatalyst caused agglomeration of catalysts, which inhibited the penetration of UV light into the MB solution as it limited the surface area accessible for light absorption (Zhang et al., 2018). As a result, the MB photocatalytic activity was hindered since the light irradiation for the reaction presented was not sufficient, which reduced the generation of electron-hole pairs (Chen et al., 2020). It is crucial to determine the optimum photocatalyst dosage to obtain complete photon absorption for effective photodegradation of MB. As for TiO2, the trend was different, most likely due to the difference in band gap energies, which might also contribute to this result as the chemical structures' complexity might affect the interaction between the photocatalysts and the degradation efficiency (Koe et al., 2019).

To summarize, it showed that the optimum photocatalyst dosage for TiO2/graphene-M2 and TiO2/graphene-M3 is 0.3 g/L, whereas for TiO2 is 0.4 g/L. In terms of the optimum mixing ratio of graphene to TiO2, TiO2/graphene-M2 achieved the highest degradation efficiency, proving that the incorporation of graphene to TiO2 enhanced the performance of photocatalytic activity.

Effects of initial concentration of MB

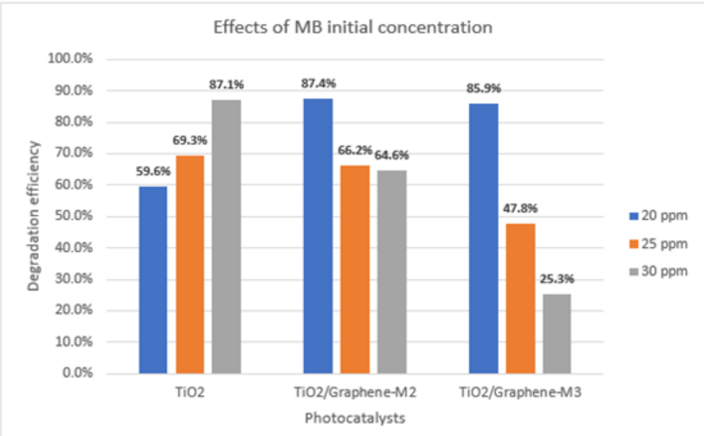

Fig. 4. Photocatalytic degradation by TiO2 and TiO2/graphene composites for different initial concentrations of MB

Fig 4 displays the influence of MB initial concentration on the photodegradation of MB. For TiO2, the degradation efficiency of MB increased from 59.6% to 87.1% as the MB initial concentration was increased from 20 ppm to 30 ppm. Next, the degradation efficiency of MB using TiO2/graphene-M2 photocatalysts was shown to be decreased (87.4% to 64.6%) as the MB initial concentration was increased from 20 ppm to 30 ppm. Lastly, TiO2/graphene-M3 also showed the same trend as TiO2/graphene-M2, with the degradation efficiency of MB recorded to be highest at 20 ppm (85.9%) while the lowest efficiency was 25.3% as the concentration was increased to 30 ppm. For TiO2, the increase in the photodegradation rate of MB with increasing initial MB concentration was due to the rise in the probability of reaction between the dye molecules and hydroxyl radicals (Anju Chanu et al., 2019). The shortage of MB molecules adsorbed on the TiO2 photocatalyst's surface led to decreased collision rates between MB dye molecules and free radicals, resulting in a low MB degradation rate (Koe et al., 2019). As MB initial concentration increased from 20 ppm to 30 ppm, a greater amount of MB was available for a higher chance of collision with hydroxyl radicals. As for TiO2/graphene-M2 and TiO2/graphene-M3, the highest degradation of MB dye was recorded at the lowest MB concentration because of the availability of more active sites on the photocatalyst's surface (Koe et al., 2019). This led to higher adsorption of MB molecules on the photocatalyst's surface and greater formation of hydroxyl radicals. The degradation efficiency decreases as MB's initial concentration increases due to the intermediate products of MB degradation, which have lower light absorbance and need to compete with MB for the reaction of hydroxyl radicals and thus reduce the efficiency of MB degradation (Xu et al., 2014).

Effects of irradiation time

Fig 5 depicts the influence of irradiation time on the MB photocatalytic degradation. It was found that during the first hour of MB degradation, the degradation rate was very high, reaching 65.3%, 66.8% and 76.8% for TiO2, TiO2/graphene-M2 and TiO2/graphene-M3, respectively. After that, the photodegradation rate of MB gradually decreased for all photocatalysts. The rapid increase in the degradation rate at the start of the process was caused by the huge formation of hydroxyl radicals. The high amount of hydroxyl radicals led to an increase in MB degradation rate since hydroxyl radicals are strong oxidizers used in degrading MB compounds (Wardhani et al., 2018). However, as the photocatalyst consumption increased, which reduced the formation rate of hydroxyl radicals, MB's degradation rate gradually decreased with an increase in time. Among these three photocatalysts, it was proven that TiO2/graphene-M2 showed the best performance as it achieved the highest degradation of MB (91.2%) after 2 hours, followed by TiO2/graphene-M3 (90.3%) and TiO2 (88.1%).

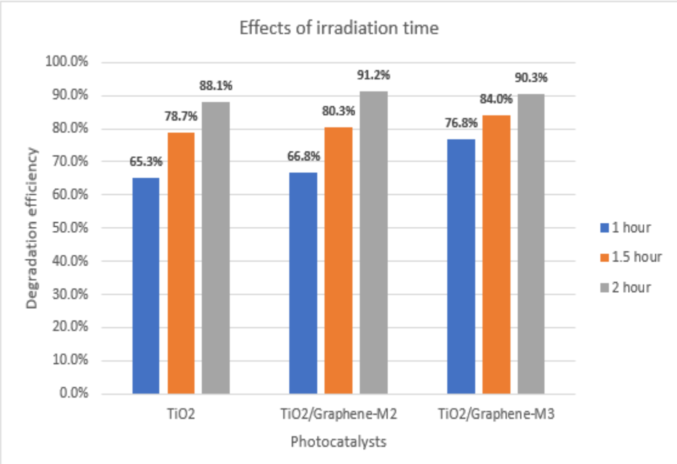

Fig. 1. Photocatalytic degradation by TiO_2 and TiO_2/graphene composites for different irradiation time

Statistical analysis of MB photocatalytic degradation

The interaction among the operational parameters, which are photocatalyst dosage, initial concentration of MB and irradiation time on the degradation efficiency of MB, was assessed by CCD using RSM. TiO2/graphene-M2 photocatalyst was selected for statistical analysis in this study. It is observed that the MB degradation efficiency ranges from 67.40 to 83.80. Thus, it can be concluded that photocatalytic degradation of MB is highly influenced by these operational parameters. Based on the experimental results, the correlations between the degradation efficiency of MB and operational parameters can be described by constructing a second-order polynomial equation, as shown in Equation (2).

Efficiency of MB degradation (%) $= 77.98 + 1.16A - 1.77B + 3.55C + 2.55\,AB + 0.2652AC - 0.0837BC - 2.50A^2 - 0.7818B^2 - 0.1244C^2$ (2)

In the above equation, A indicates photocatalyst dosage, B is MB initial concentration, and C is irradiation time. The positive and negative sign in front of the equation represents the synergistic effect (increase in the percentage of MB removal) and antagonistic effect, respectively.

The actual and predicted values of MB degradation efficiency are illustrated in Table 5 and Fig. 6. The result indicated a very high correlation between the experimental and the predicted values, which further supports the good predictability of the model.

Tab. 5. Central composite design with actual and predicted MB degradation efficiency

Run	Factor 1	Factor 2	Factor 3	MB Degradation Efficiency (%)	
	Photocatalyst Dosage (g/L)	Initial Concentration MB (ppm)	Irradiation time (min)	Actual	Predicted
1	0.2	30	120	72.18	72.29
2	0.4	30	60	72.70	72.78
3	0.3	25	90	78.38	77.98
4	0.3	16.59	90	78.07	78.75
5	0.4	20	120	78.03	78.85
6	0.2	20	60	75.00	74.37
7	0.3	25	90	77.85	77.98
8	0.4	20	60	72.12	71.06
9	0.3	25	90	76.99	77.98
10	0.2	30	60	67.66	65.89
11	0.3	25	90	77.33	77.98
12	0.47	25	90	73.02	72.85
13	0.3	25	39.55	70.11	71.66

14	0.2	20	120	82.13	81.10
15	0.3	25	140.45	83.80	83.59
16	0.13	25	90	67.44	68.95
17	0.3	25	90	78.21	77.98
18	0.3	25	90	79.35	77.98
19	0.4	30	120	80.55	80.23
20	0.3	33.41	90	72.12	72.79

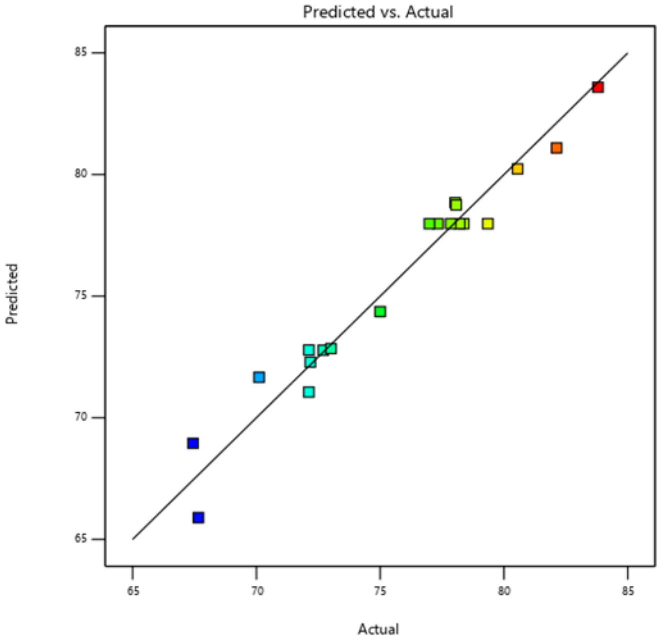

Fig. 6. Predicted value vs the Actual value for MB degradation efficiency

The analysis of variance (ANOVA) was obtained for the modified regression model to analyze data and evaluate the fitted model's quality (Bezerra et al., 2008). The ANOVA for MB degradation was generated by calculating the F-value, p-value, sum of squares, mean square and the degree of freedom, as shown in Table 6

Tab. 6. Analysis of variance (ANOVA) of the quadratic model for MB degradation

Source	Sum of Squares	DF	Mean Square	F-value	p-value	
Model	380.35	9	42.26	26.97	<0.0001	Significant
A - Photocatalyst dosage	18.32	1	18.32	11.69	0.0066	
B - Initial concentration of MB	42.86	1	42.86	27.36	0.0004	
C - Irradiation time	171.74	1	171.74	109.62	<0.0001	
AB	51.95	1	51.95	33.16	0.0002	
AC	0.5629	1	0.5629	0.3593	0.5623	
BC	0.0561	1	0.0561	0.0358	0.8537	
A^2	90.28	1	90.28	57.62	<0.0001	
B^2	8.81	1	8.81	5.62	0.0392	
C^2	0.2230	1	0.2230	0.1432	0.7138	
Residual	15.67	10	1.57			
Lack of Fit	12.17	5	2.43	3.48	0.0986	Not significant
Pure Error	3.50	5	0.6991			
Cor Total	396.02	19				

Std. Dev	1.25	**R^2**	0.9604
Mean	75.65	**Adjusted R^2**	0.9248
C.V.%	1.65	**Predicted R^2**	0.7441
		Adeq Precision	19.9943

The model's F-value of 26.97 indicated that it was statistically significant, with less than a 0.01% chance that it might occur as a result of noise. The value of the correlation coefficient R2 was determined to be 0.9604, which is close to unity (1), further confirming the model's fitness in predicting the experimental values of the response (Anju Chanu et al., 2019). This also suggested that the variation of 96.04% for MB degradation was explicated with the aid of independent factors within the studied range (Lee et al., 2015). In addition, the lack of fit for this model was found to be not significant relative to pure error, as the p-value of 0.0986 is greater than 0.05. This represents a good predictability of the model. Furthermore, the small coefficient of variation (CV=1.65) implied high precision and good predictability of experimental results.

Another important measure to describe the variation in this fitted model is adequate precision, which calculates the signal-to-ratio noise. Adeq Precision of 19.9943 indicated an adequate signal as it is greater than 4 (Shukor et al., 2022). Thus, ANOVA results suggested that the model is desirably fit and is a reliable approach to represent the relationship between the photocatalyst dosage, MB initial concentration, and irradiation time with the degradation efficiency of MB.

Interactions between operational parameters

In this study, the interaction between photocatalyst dosage and MB initial concentration (AB) was studied since this two-level interaction model is proven to be significant. Fig 7. and Fig 8. showed the three-dimensional (3D) surface plot and contour plot, respectively, for the interaction of photocatalyst dosage and MB initial concentration on the degradation of MB. It showed that increasing the photocatalyst dosage led to a higher percentage of MB removal until it reached the critical limit of 0.3 g/L. On the other hand, the initial concentration affected the MB removal differently, as the highest efficiency of MB photodegradation was achieved at the lowest initial concentration of MB (20 ppm).

Based on the plot that, with decreasing MB concentration, an increase in photocatalyst dosage had a proportional effect on MB degradation efficiency until it reached the critical limit. This might have happened due to the availability of more active sites on the photocatalyst's surface, which led to higher adsorption of MB molecules and greater formation of hydroxyl radicals (Koe et al., 2019).

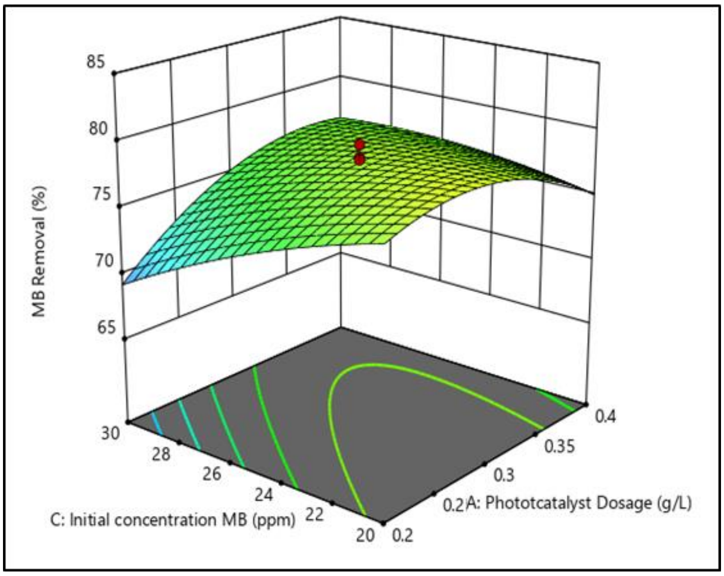

Fig. 7. 3D surface plot of interaction AB

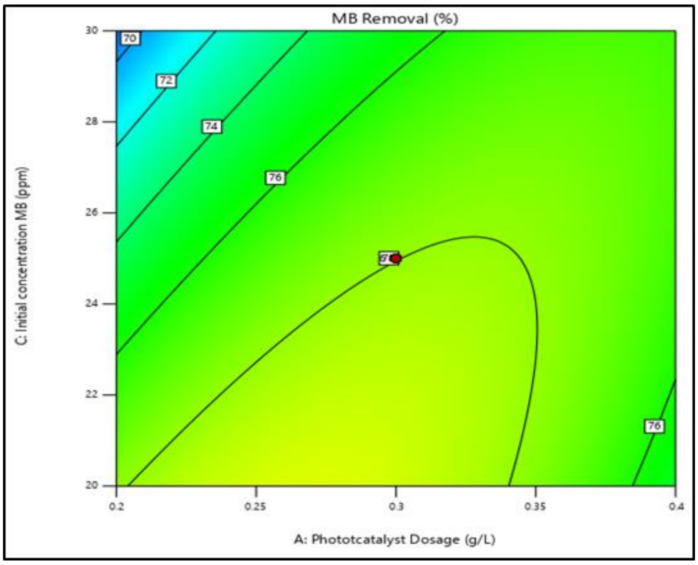

Fig. 8. Contour plot of interaction AB

Conclusions

The synthesis of TiO_2/graphene composites was carried out to study their characterization and applied as the photocatalysts for the degradation of methylene blue (MB). The functional groups of the photocatalysts were shown in the results of FTIR analysis, confirming the presence of graphene and TiO_2 in the synthesized photocatalysts. The XRD analysis showed that the combination of TiO_2 and graphene using the wet-impregnation method did not affect the crystalline structure of the photocatalyst. The results found that photocatalyst dosage and irradiation time had similar trends as they were directly proportional to the degradation efficiency until it reached the optimum value. On the other hand, the initial concentration of MB for TiO_2/graphene-M2 and TiO_2/graphene-M3 showed the opposite trend as it was inversely proportional to the degradation efficiency except for TiO_2 photocatalyst, which might happen due to different band gap energy. TiO_2/graphene-M2 was proven to be the most efficient photocatalyst with a mass ratio of 50:50 as it exhibited the highest efficiency of MB photodegradation compared to TiO_2 and TiO_2/graphene-M2. Increasing the ratio of graphene reduced the band gap, leading to a better absorption ability in UV light and thus improving the photocatalytic activity. The experimental design of MB photocatalytic degradation was carried out by selecting TiO_2/graphene-M2 to determine the significance of the model for the MB photodegradation using response surface methodology. From the analysis, it can be concluded that the model is highly significant in the MB degradation as the p-values are less than 0.05.

Overall, TiO_2/graphene is capable of becoming an efficient photocatalyst that can be used for the degradation of MB. The incorporation of graphene into TiO_2 enhanced the performance of photocatalytic degradation of organic pollutants for environmental remediation.

References

Abdel-Khalek AA, Mahmoud SA, Zaki AH (2018). Visible light assisted photocatalytic degradation of crystal violet, bromophenol blue and eosin Y dyes using AgBr-ZnO nanocomposite. Environmental Nanotechnology, Monitoring and Management 9 (March) :164–173. https://doi.org/10.1016/j.enmm.2018.03.002

Amali Z, Ramli C, Asim N, Isahak, WNRW, Emdadi Z, Ahmad-ludin N, Yarmo M.A, Sopian K (2014). *Photocatalytic Degradation of Methylene Blue under UV Light Irradiation on Prepared Carbonaceous TiO2 2014*(C): 13–15.

Anju Chanu L, Joychandra Singh W, Jugeshwar Singh K, Nomita Devi K (2019). Effect of operational parameters on the photocatalytic degradation of Methylene blue dye solution using manganese doped ZnO nanoparticles. Results in Physics 12: 1230–1237. https://doi.org/10.1016/j.rinp.2018.12.089

Bezerra MA, Santelli RE, Oliveira EP, Villar LS, Escaleira LA (2008). Response surface methodology (RSM) as a tool for optimization in analytical chemistry. Talanta 76(5): 965–977. https://doi.org/10.1016/j.talanta.2008.05.019

Chen D, Cheng Y, Zhou N, Chen P, Wang Y, Li K, Huo S, Cheng P, Peng P, Zhang R, Wang L, Liu H, Liu Y, Ruan R (2020). Photocatalytic degradation of organic pollutants using TiO2-based photocatalysts: A review.

Journal of Cleaner Production 268: 121725. https://doi.org/10.1016/j.jclepro.2020.121725
Dao HM, Whang CH, Shankar VK, Wang YH, Khan IA, Walker LA, Husain I, Khan SI, Murthy SN, Jo S (2020). Methylene blue as a far-red light-mediated photocleavable multifunctional ligand. Chemical Communications 56(11): 1673–1676. https://doi.org/10.1039/c9cc08916k
Durango-Giraldo G. Cardona A, Zapata JF, Santa JF, Buitrago-Sierra R (2019). Titanium dioxide modified with silver by two methods for bactericidal applications. Heliyon 5(5) e01608. https://doi.org/10.1016/j.heliyon.2019.e01608
Fang W, Xing M, Zhang J (2017). Modifications on reduced titanium dioxide photocatalysts: A review. Journal of Photochemistry and Photobiology C: Photochemistry Reviews 32: 21–39. https://doi.org/10.1016/j.jphotochemrev.2017.05.003
Gaikwad RW, Sapkal VS and Sapkal RS (2010). Acta Montanistica Slovaca Volume 15, number 4, 298-304
Hana K, Vladislav S, Kristína G, Igor W, Yury N, Lenka B and Maroš S (2017). The Use of Waste From Bauxite Ore in Sorption of 3,5-Dichlorophenol From Waste Water. Acta Montanistica Slovaca Volume 22, number 4, 404-411
Hou C, Hu B, Zhu J (2018). Photocatalytic degradation of methylene blue over TiO2 pretreated with varying concentrations of NaOH. Catalysts 8(12). https://doi.org/10.3390/catal8120575
Juraj M, Veronika K, Kristína S, Alexandra K and Maros S (2021). The Usage of Red Mud and Black Nickel Mud. Acta Montanistica Slovaca, Volume 26, Number 3, 546-554
for Removal of Methylene Blue
Khalid NR, Majid A, Tahir MB, Niaz NA, Khalid S (2017). Carbonaceous-TiO2 nanomaterials for photocatalytic degradation of pollutants: A review. Ceramics International 43(17): 14552–14571. https://doi.org/10.1016/j.ceramint.2017.08.143
Koe WS, Lee JW, Chong WC (2019). An overview of photocatalytic degradation : photocatalysts , mechanisms , and development of photocatalytic membrane.
Lee KM, Abdul Hamid SB, Lai CW (2015). Multivariate analysis of photocatalytic-mineralization of Eriochrome Black T dye using ZnO catalyst and UV irradiation. Materials Science in Semiconductor Processing 39: 40–48. https://doi.org/10.1016/j.mssp.2015.03.056
Li H, Ji J, Cheng C, Liang K (2018). Preparation of phenol-formaldehyde resin-coupled TiO2 and study of photocatalytic activity during phenol degradation under sunlight. Journal of Physics and Chemistry of Solids 122: 25–30. https://doi.org/10.1016/j.jpcs.2018.06.012
Li Y, E T, Liu L, Yang S, Qian J, Ma Z (2020). Preparation of needle-like TiO2/Graphene for electrical conductive analysis. Journal of Materials Science 55(2): 670–679. https://doi.org/10.1007/s10853-019-04044-z
Liu C, Zhang L, Liu R, Gao Z, Yang X, Tu Z, Yang F, Ye Z, Cui L, Xu C, Li Y (2016). Hydrothermal synthesis of N-doped TiO2 nanowires and N-doped graphene heterostructures with enhanced photocatalytic properties. Journal of Alloys and Compounds 656: 24–32. https://doi.org/10.1016/j.jallcom.2015.09.211
Mahalingam S, Durai M, Sengottaiyan C, Ahn Y-H (2021). Effective Chemical Vapor Deposition and Characterization of N-Doped Graphene for High Electrochemical Performance. Journal of Nanoscience and Nanotechnology 21(6): 3183–3191. https://doi.org/10.1166/jnn.2021.19355
Muhd Julkapli N, Bagheri S, Bee Abd Hamid S (2014). Recent advances in heterogeneous photocatalytic decolorization of synthetic dyes. Scientific World Journal 2014. https://doi.org/10.1155/2014/692307
Najafi M, Kermanpur A, Rahimipour MR, Najafizadeh A (2017). Effect of TiO2 morphology on structure of TiO2-graphene oxide nanocomposite synthesized via a one-step hydrothermal method. Journal of Alloys and Compounds 722: 272–277. https://doi.org/10.1016/j.jallcom.2017.06.001
Nasir A, Khalid S, Yasin T, Mazare A (2022). A Review on the Progress and Future of TiO2/Graphene Photocatalysts. In: Energies (Vol. 15, Issue 17). https://doi.org/10.3390/en15176248
Nasir A, Raza A, Tahir M, Yasin T(2020). Free-radical graft polymerization of acrylonitrile on gamma irradiated graphene oxide: Synthesis and characterization. Materials Chemistry and Physics 246. https://doi.org/10.1016/j.matchemphys.2020.122807
Ouyang W, Zeng D, Yu X, Xie F, Zhang W, Chen J, Yan J, Xie F, Wang L, Meng H,Yuan D (2014). Exploring the active sites of nitrogen-doped graphene as catalysts for the oxygen reduction reaction. International Journal of Hydrogen Energy 39(28): 15996–16005. https://doi.org/10.1016/j.ijhydene.2014.01.045
Shukor H, Yaser AZ, Shoparwe NF, Mohd Zaini Makhtar M, Mokhtar N (2022). Biosorption Study of Methylene Blue (MB) and Brilliant Red Remazol (BRR) by Coconut Dregs. International Journal of Chemical Engineering 2022. https://doi.org/10.1155/2022/8153617
Sun L, Hu D, Zhang Z, Deng X (2019). Oxidative degradation of methylene blue via PDS-based advanced oxidation process using natural pyrite. International Journal of Environmental Research and Public Health, 16(23). https://doi.org/10.3390/ijerph16234773
Sun M, Kong Y, Fang Y, Sood S, Yao Y, Shi J, Umar A (2017). Hydrothermal formation of N/Ti3+ codoped multiphasic (brookite-anatase-rutile) TiO2 heterojunctions with enhanced visible light driven photocatalytic performance. Dalton Transactions 46(45): 15727–15735. https://doi.org/10.1039/c7dt03268d

Wardhani S, Purwonugroho D, Fitri CW, Prananto YP (2018). Effect of pH and irradiation time on TiO2-chitosan activity for phenol photodegradation. AIP Conference Proceedings 2021(2018). https://doi.org/10.1063/1.5062759

Xu C, Rangaiah GP, Zhao XS (2014). Photocatalytic degradation of methylene blue by titanium dioxide: Experimental and modeling study. Industrial and Engineering Chemistry Research 53(38): 14641–14649. https://doi.org/10.1021/ie502367x

Zhang J, Tian B, Wang L, Xing M, Lei J (2018). *Mechanism of Photocatalysis*. 1–15. https://doi.org/10.1007/978-981-13-2113-9_1